IEEE Photonics Journal
An IEEE Photonics Society Publication

Open Access

Spatially Resolved Brillouin Spectral Hole Burning in PMF and SMF

Volume 10, Number 4, August 2018

Xiaoxuan Zhong
Hao Liang
Linghao Cheng
Jie Li
Liang Chen
Xiaoyi Bao
Bai-ou Guan

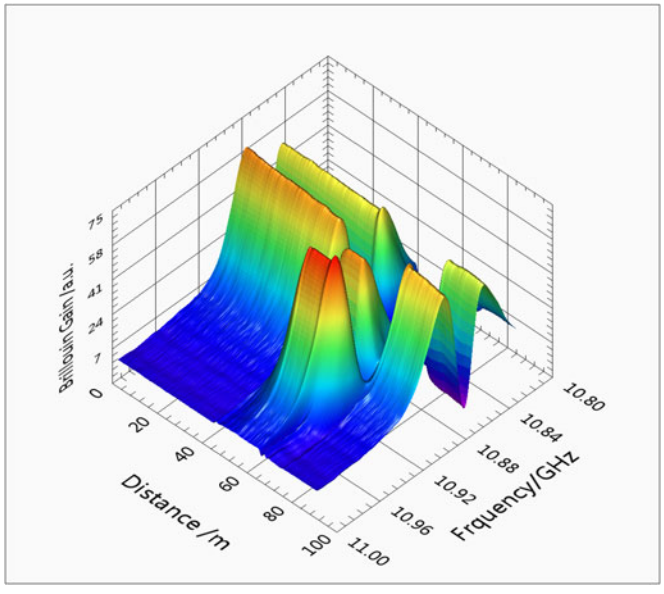

DOI: 10.1109/JPHOT.2018.2853154
1943-0655 © 2018 IEEE

IEEE photonics SOCIETY

IEEE

Spatially Resolved Brillouin Spectral Hole Burning in PMF and SMF

Xiaoxuan Zhong,[1] Hao Liang,[1] Linghao Cheng,[1] Jie Li,[1] Liang Chen,[2] Xiaoyi Bao,[2] and Bai-ou Guan [1]

[1]Guangdong Provincial Key Laboratory of Optical Fiber Sensing and Communications, Institute of Photonics Technology, Jinan University, Guangzhou 510632, China
[2]Fiber Optics Laboratory, Department of Physics, University of Ottawa, Ottawa, ON K1N 6N5, Canada

DOI:10.1109/JPHOT.2018.2853154

Manuscript received March 20, 2018; revised June 19, 2018; accepted June 28, 2018. Date of publication July 5, 2018; date of current version July 16, 2018. This work was supported by the National Natural Science Foundation of China under Grants 61307100, 61675091, and 61575083. Corresponding author: H. Liang (e-mail: lianghao1509@gmail.com).

Abstract: We observe the spectral hole burning effect in a polarization maintain fiber (PMF) and a single-mode fiber (SMF) through the interaction between a continuous wave (CW) beam and a high power pulse with two frequency components located around the Stokes and anti-Stokes frequencies of the CW beam. The linewidth of the spectral burning hole is much narrower than that of the intrinsic Brillouin gain spectrum. We experimentally study the position dependent dip formation process in a PMF and an SMF, and explore the possibility of using this narrowed spectral width for distributed temperature and strain sensing with a higher accuracy. A hole burning peak with a linewidth of 9 MHz in a Brillouin gain spectrum with a full-width at half-maximum (FWHM) of 50 MHz is observed in a PMF. Since the frequency measurement accuracy of Brillouin sensor is inversely proportional to the FWHM of detected spectrum, the spectrum hole burning represents a potential for improving the Brillouin peak detection accuracy of distributed Brillouin sensor.

Index Terms: Brillouin scattering, spectral hole burning, temperature and strain sensing, optical fiber sensor.

1. Introduction

Distributed optical fiber sensors based on Brillouin scattering have been studied for more than two decades. They have great potentials in industrial applications to smart materials and structures, because they can provide a distributed temperature and strain measurement over a long distance by measuring the frequency shift of Brillouin power spectrum [1]–[9]. It has been shown that the peak-power frequency-measurement accuracy is inversely proportional to the full width at half-maximum (FWHM) of the detected spectrum [10], [11]. Although a long probe pulse might lead to a narrow spectrum, the narrowest FWHM cannot be less than that of the intrinsic Brillouin gain spectrum determined by phonon damping rate.

Recently, the spectral hole burning introduced by gain saturation and the coupling between pump and probe signal perturbations has been observed in Brillouin fiber amplifiers [12]–[14]. It has been demonstrated to give a narrow dip at the resonance frequency in Brillouin gain region, and the depth and width of the dip depends on the pump power and fiber length. In this mechanism, a strong pump light and Stokes light counter propagated in the optical fiber, the saturation gain

spectrum is recorded by measuring the gain of a weak probe signal with frequency scanning within the Brillouin gain region. Since the gain of the weak probe signal is limited by the coupling with the strong Stokes light at the Brillouin resonance peak frequency, a relatively higher gain can be observed at the off-resonance frequencies due to lower gain coefficient comparing with that at the original peak resonance. As a result, a dip is formed around center frequency of the Brillouin gain [12]. However, because of the weak probe signal, the current hole burning observation technique leads to a low SNR, and the spectra is observed for the entire fiber without location information obtained. It means that the evolution of this hole burning along the fiber cannot be achieved. In this paper, we proposed a new distributed Brillouin gain hole burning detection method based on time domain analysis through the interaction between the Stokes-directed absorption and the anti-Stokes-directed scattering. In this method, a dip is observed at the resonance frequency of the Brillouin gain by detecting the power change of the probe continuous wave (CW) beam counter-propagated with two pulses of frequency scanning around Stokes and anti-Stokes resonance of the CW beam, respectively. It is demonstrated through experiments that Brillouin spectral hole burning effect can be observed without invoking the gain saturation described in [12], The dip in the spectrum can be sharpened if the pump and probe power is optimized, and a relatively high SNR can be achieved. In the experiment, when the pulsewidth is much greater than the phonon life time, a narrow dip with a linewidth about 10 MHz is observed in the Brillouin spectrum of PMF and SMF. As this dip frequency is coincident with the central peak Brillouin frequency, and is sensitive to temperature and strain, it provides a new alternative for high accuracy distributed temperature and strain measurement.

2. Observation of Brillouin Spectral Hole Burning

Stimulated Brillouin scattering (SBS) is a parametric process involving a pump beam, a Stokes beam, and an acoustic wave. SBS occurs when two coherent light waves with a frequency difference at the acoustic frequency counter-propagates in a fiber. In this process, the power is transferred from pump light at a higher frequency to Stokes light at a lower frequency through acoustic wave [16]. Consider a situation where an optical CW beam counter-propagates with an optical pulse containing two frequency components located at the Stokes and the anti-Stokes resonance frequency of the CW beam respectively, as shown in Fig. 1(a), the CW beam might experience Brillouin gain and loss process simultaneously. Taking the CW beam as probe wave, it means the power might be transferred from anti-Stokes wave to probe wave and from probe wave to Stokes wave simultaneously. If the frequency of the pulse is scanned around Brillouin resonance frequencies, a coherent Brillouin gain and loss spectrum can be recorded by detecting the intensity change of the CW beam at different frequencies as shown in Fig. 1(b). In the absence of the low-frequency pulse component, the high-frequency beam will experience strongly resonance absorption to the probe CW beam when these two beams satisfy the Brillouin phase matching condition. In this process the energy of the CW beam increases as the blue line in Fig. 1(b). Similarly, a loss process can be expected for the CW beam when there is low-frequency pulse component only. Intuitively, when pulse with two frequency components are presented, the intensity of the CW beam should have little fluctuation over frequency due to the balance between gain and loss. At the same time, the depletion of the high-frequency component should be greater, because its energy could transfer to the CW beam and then to the low-frequency pulse component through SBS process. However, theoretically, the anti-Stokes-directed scattering path might be established in Brillouin scattering process [17], [18]. In this case, the low-frequency mode could coherently couple to the high-frequency mode resulting a previously unforeseen transparency at the frequency $\omega_0 + \Omega_{as}$, corresponding to a narrow dip at ω_0 in the spectrum recorded by the intensity variation of the CW light.

To observe the gain hole burning spectra distributedly, an experimental setup as shown in Fig. 2 is used. A beam of CW at 1550 nm is split into two parts by a coupler. One is injected into the fiber under test (FUT) through an isolator (ISO) as the probe CW. The other is modulated by an electro-optic modulator (EOM) driven by a microwave synthesizer at angular frequency Ω_{RF} and gated to a pulse. Thus the pulse contains two frequency components with the same amplitude and

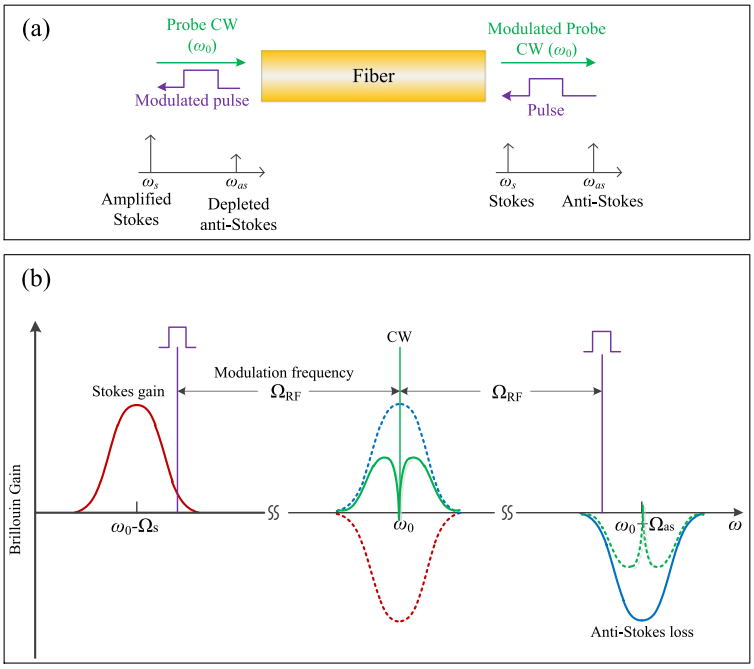

Fig. 1. (a) is configuration for observe Brillouin spectrum hole burning and frequency location of CW probe and pulsed light, (b) is Schematic relationships in the light frequencies. In traditional SBS theory, gain and loss for CW light at ω_0 through SBS could cancel each other. However, because of the interference between Stokes and anti-Stokes scattering pathway, a hold burning spectrum might be observed.

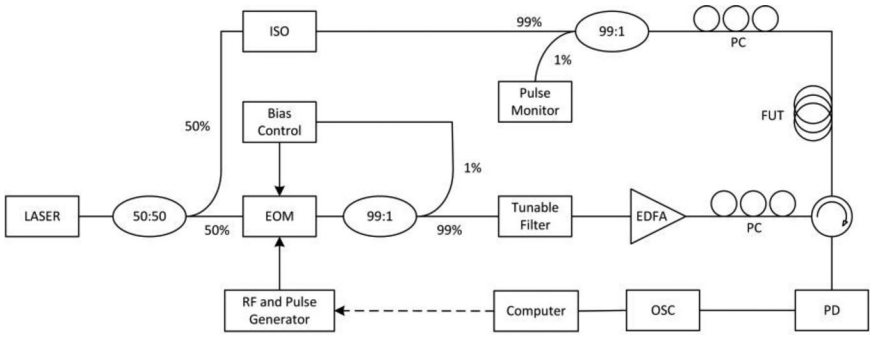

Fig. 2. Experimental setup of the accuracy enhanced distributed Brillouin sensor system.

polarization state. A modulator bias controller is used to generate a high pulse extinction ratio(ER). The pulse amplified by an Erbium doped fiber amplifier (EDFA) is launched into the other end of FUT through a circulator and its shape is obtained by a pulse monitor. The intensity of the probe light is detected by a photodetector (PD) and then recorded as time traces by a digital oscilloscope (OSC). Polarization controllers (PCs) are used to modulate the polarization states of light beams to obtain a high SBS efficiency. The tunable filter is used to select the frequency component of the pulse.

In the experiment, the pulsewidth, peak power and ER for the pulsed signal are 50 ns, 500 mW and 30 dB respectively. And the power of the counter propagated CW light is about 5 mW. Fig. 3(a) and (b) shows the distribution of the hole burning spectrum in a 100 m PMF and a 100 m SMF respectively. In both fibers, spectra with burning hole at the Brillouin resonance frequency are

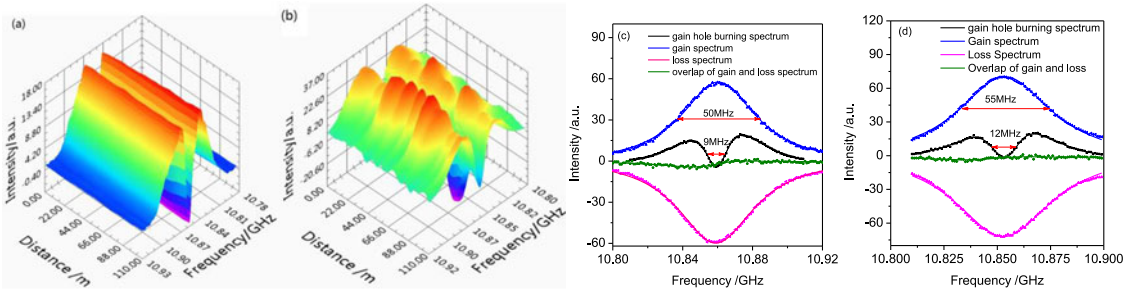

Fig. 3. (a) and (b) are spectrum distribution in a 100 m PMF and a 100 m SMF respectively, (c) and (d) are comparison of the hole burning spectrum and the Brillouin gain and the loss spectra in the PMF and the SMF respectively.

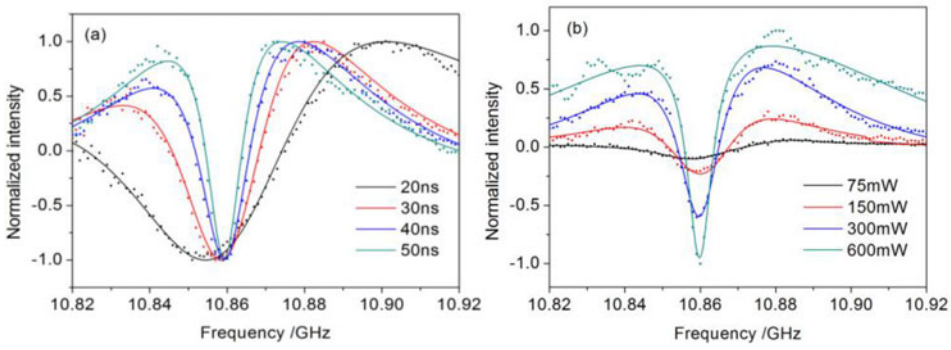

Fig. 4. (a) is spectra measured in the PMF by using a 500 mW pulse with different pulsewidth, (b) is spectra measured in the PMF by using a 50 ns pulse with different peak power.

achieved. The intensity fluctuation of the SMF spectra is caused by polarization mode dispersion (PMD). Black curve in Fig. 3(c) and (d) shows the detected spectrum located at 80 m of the PMF and SMF respectively. It can be seen that the linewidth of the dip is about 9 MHz for PMF. Due to the inhomogeneous of the fiber, the linewidth of the dip in SMF is 3 MHz larger than that in PMF, and it slightly varies along the fiber. When the frequency of the RF is scanned from 10.8 GHz to 10.9 GHz, the intensity of the CW light firstly experiences a gain process and rapidly changes to a loss process at around the resonance peak frequency before coming to the gain process again. To compare with the conventional Brillouin spectrum, the two sidebands of the pulse are filtered out in turn using a tunable band pass filter before they interact with the CW light in the fiber. Then we obtain the Brillouin gain and the loss spectra separately at the same location as described by the blue and pink line in Fig. 3(c) and (d). It is indicated that both the Brillouin gain spectrum and the loss spectrum follow Lorentzian shape. Because of the chromatic dispersion of the fiber, the center frequency of the loss spectrum is about 1 MHz less than that of the gain spectrum. Their FWHMs are about 50 MHz for PMF and 55 MHz for SMF, which are common but more than 5 times larger than that of the burning hole. The summation of the gain and the loss spectra is presented as the green curves in Fig. 3(c) and (d). Obviously, the maximum intensity change of the detected spectra with hole burning is much larger than that obtained by the summation of the gain and loss spectra. The peak intensity of the spectra with hole burning is about 1/3 of conventional Brillouin gain peaks. It indicates that when the two frequency pulse components and the CW light beam satisfy phase matching condition with acoustic modes simultaneously, the anti-Stokes-directed scattering path might be established in this process. Similar to the Brillouin induced transparency reported in [17], [18], a narrow dip can then be observed in the Brillouin spectrum.

TABLE 1
Linewidth of the Dip Under Different Pulsewidth

Pulsewidth /ns	20	30	40	50
Linewidth /MHz	52.1	22.3	14.5	8.9

TABLE 2
Linewidth of the Dip Under Different Pulsewidth

Pulsepower /mW	75	150	300	600
Linewidth /MHz	29.5	18.2	11.9	8.1

To further study the requirement for the Brillouin gain hole burning effect, we kept the CW light power at 5 mW, and detected spectra under different pulsewidth and pulse peak power and fitted the data using transmission profile model of electromagnetically induced transparency (EIT) described in [19]. To avoid PMD of the fiber, we use a PMF as FUT in the experiment. Fig. 4(a) shows the spectra measured by using a 500 mW pulse with different pulsewidth. It can be seen that the shape of the detected spectrum various as the pulsewidth changes. From Table 1, as the pulsewidth increases, the linewidth of the spectral hole decreases. We also detected the spectra in a short fiber with a length of 2 m. It is found that even a 50 ns pulse with a power of 500 mW is used, the SNR of the spectrum observed in the short fiber is lower than that in the long fiber, and the two gain regions are asymmetric which is similar to those detected by using short pulses. It means that the spectral hole burning is easier to happen at steady state, where the interaction time of the counter propagated lights is much larger than the phonon life time. Fig. 4(b) shows the spectra with different peak power when the pulsewidth is kept at 50 ns. It can be seen that the depth of the dip increases as pulse power rises. It is indicated that the hole burning effect observed is not simply originated from gain saturation described in [12]–[14]. Moreover, intensity fluctuation appears in the gain region of the spectrum when the pulse power is increased to about 600 mW. It may be attributed by modulation instability caused by high power. The measured linewidth of the dip under different pulsewidth and power is list in Tables 1 and 2 respectively. It is demonstrated that the dip in the spectrum can be sharpened with large pulse pulsewidth and peak power.

Since the pulse power might change the shape of the dip, we use a 1 km single mode fiber (SMF) in loose state as FUT to study the influence of the pump depletion to the hole burning effect. A 500 ns pulse with a peak power of about 300 mW and a CW beam with a power of 5 mW are launched into fiber. We measured the spectra distributedly with the setup shown in Fig. 3. Fig. 5(a) shows the evolution of the hole burning along the fiber. The fluctuation of the intensity is caused by PMD of the SMF. Fig. 5(b) is the spectra obtain at different positions of the FUT. The gain of the spectra with hole burning is shown to decrease along the fiber while the loss at the center frequency of the dip increases. The linewidth of the spectrum at 900 m is 1 MHz larger than that at 100 m. It might be due to the depletion of the pulse component at $\omega_0 + \Omega_{RF}$ through SBS process. Through a conventional BOTDA with the same pulse and CW power, the Brillouin gain spectra distribution in the fiber at the same positions as those in Fig. 5(b) was obtained and shown in Fig. 5(c) for comparison. The Brillouin gain spectrum obtained by conventional BOTDA method follows Lorentz shape at the near end of the fiber, while those obtained at far end of the fiber have a flat top. The distortion of the gain spectra then suggests that the pump and probe signal work at weak saturation region as described in [13]. We also detected the intensity variation of the transmitted pulses through the proposed setup and conventional BOTDA, respectively. As shown in Fig. 5(d), in conventional BOTDA system, the depletion of the pulse reaches its maximum at the Stokes resonance of CW beam of around 10.86 GHz, and it roughly follows the Lorentz shape. By using

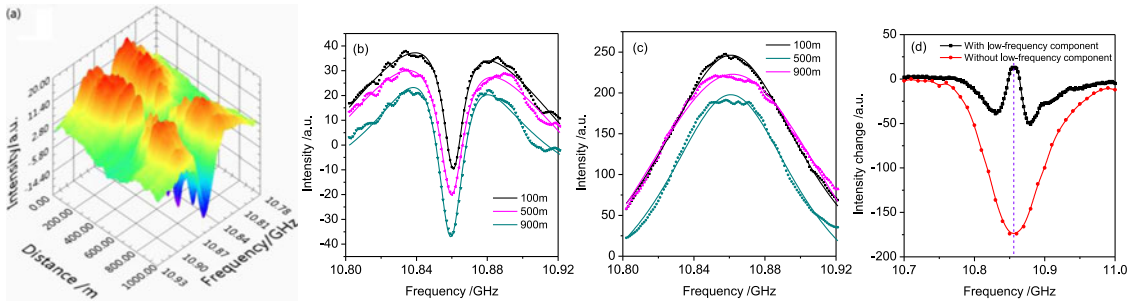

Fig. 5. (a) is distribution of the hole burning spectra along a SMF fiber, (b) and (c) are hole burning spectrum and gain spectrum at different position of the fiber respectively and (d) is comparison of intensity change of the transmitted pulse in PMF and SMF.

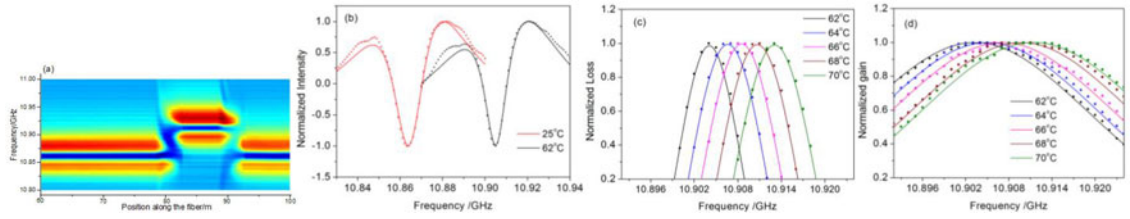

Fig. 6. (a) Spectrum distribution along the fiber. (b) Measured spectra of Brillouin gain hole burning under different temperature (c) spectrum variation of Brillouin spectral hole (d) spectrum variation of Brillouin gain.

the setup in Fig. 3, in presence of the pulse component at $\omega_0 - \Omega_{RF}$, the depletion of the pulse at the high frequency of $\omega_0 + \Omega_{RF}$ decreases with a minimal depletion at the resonance frequency, which means the pulse energy no longer couples into the CW beam as it would be expected. The hole burning in Brillouin spectrum should therefore be a result of the coherent interaction between the Stokes-directed absorption and anti-Stokes-directed scattering, rather than a simple combination of Brillouin gain and loss spectrum or gain saturation.

3. Temperature and Strain Sensing Experiment and Discussion

Since the frequency of the burning hole in the spectrum is coincident with the resonance peak of Brillouin spectrum, it should be sensitive to temperature and strain. In experiments, PMF is used for measurement with a section of 10 m in an oven. The temperature of the oven is varied from 62 °C to 70 °C in a step of 2 °C. The setup in Fig. 3 is used to measure the distributed temperature changes. Fig. 6(a) is the distribution of the frequency spectrum along the fiber. Fig. 6(b) shows the spectrum at the section under room temperature (25 °C) and in the heated oven. The spectral shape shows little dependence on temperature and the resonance frequency shift is proportional to temperature. Compared to conventional BOTDA technique, as shown in Fig. 6(c) and Fig. 6(d), the frequency shift is easier to be detected with high precision for its narrower linewidth. Fig. 7 exhibits the variation of the resonance frequency of the spectral hole and the Brillouin gain. Both of them increase linearly with rising temperature. The temperature and strain coefficient of the Brillouin frequency shift obtained by spectrum hole burning is 1.11 MHz/°C and 0.0498 MHz/$\mu\varepsilon$ respectively. The coefficients obtained by conventional BOTDA technique are 1.04 MHz/°C and 0.0497 MHz/$\mu\varepsilon$, respectively, which are quite close to those of spectrum hole burning.

Normally the Brillouin frequency shift has a linear dependence on temperature and strain. The Brillouin frequency accuracy is co-determined by the FWHM of the Brillouin spectrum $\Delta\nu_B$ and the

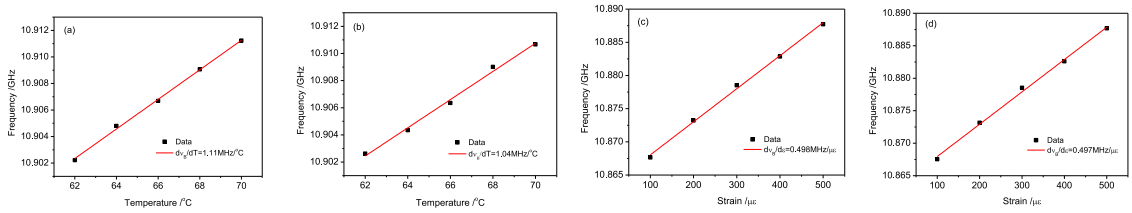

Fig. 7. Temperature dependence on Brillouin frequency shifts of Brillouin spectral hole (a), the conventional Brillouin gain (b) and strain dependence on Brillouin frequency shifts of Brillouin spectral hole (c), the conventional Brillouin gain (d).

electrical SNR.

$$\delta\nu_B = \Delta\nu_B / \left(\sqrt{2} SNR^{1/4}\right) \tag{1}$$

According to Eq. (1), a smaller FWHM results in higher frequency accuracy. The frequency uncertainty of spectrum hole burning in the experiment is calculated to be $\pm$0.47 MHz, corresponding to a temperature accuracy of $\pm$0.4 °C and a strain accuracy of $\pm$9 $\mu\varepsilon$. The frequency uncertainty of the conventional BOTDA technique is calculated to be $\pm$0.9 MHz corresponding to a temperature accuracy of $\pm$0.9 °C and a strain accuracy of $\pm$18 $\mu\varepsilon$. The frequency measurement precision improves twice through spectral hole burning effect in comparison with that through pure Brillouin gain of conventional BOTDA. According to Eq. (1), the frequency-shift precision should be improved by 5 times if the SNR is maintained as constant. However, because of the lower gain on the CW light, the spectrum has a relatively lower SNR. According to the relationship described in [11], the SNR of the hole burning spectrum is about 1/3 of the conventional Brillouin gain obtained by the same pulse power without gain saturation. Thus the improvement of the frequency-shift precision in the experiment is not as large as it would be expected. The measurement accuracy might be further improved through increasing light power or average number.

4. Conclusion

A method to induce hole burning in Brillouin gain spectrum is proposed through the interaction between Brillouin Stokes and anti-Stokes scattering, which enables time domain analysis to be adopted for distributed measurement. The influence of the pulsewidth and power to the Brillouin hole burning effect, as well as the evolution of the burning hole along the fiber is explored. In the experiment, a narrow dip with a linewidth about 10 MHz is observed around the resonance frequency of a Brillouin gain spectrum with a FWHM of about 50 MHz in the PMF. Temperature and strain measurement of the dip in the Brillouin spectrum has been demonstrated. The accuracy of peak frequency detection is calculated to be $\pm$0.47 MHz, corresponding to $\pm$0.4 °C and $\pm$9 $\mu\varepsilon$ along a 100 m PMF in the experiment, which is twice of that obtained by conventional BOTDA. It provides a new alternative for high accuracy distributed temperature and strain measurement. In particular, the interpretation of this spectral hole burning in Brillouin spectrum should be very different from those proposed in Brillouin generator or amplified as [12]–[14] based on SBS gain saturation. Moreover, although the observed hole burning phenomenon in this paper is similar to those due to EIT effect suggested by [17]–[19], one significant qualitative difference must be underlined. That is, EIT is a result of Fano interference realized in two-oscillator model with different damping. However, currently our experiment setup cannot verify that the damping of Stokes process and anti-Stokes process are different and therefore a new experiment should be carried out to further explore this issue.

References

[1] M. Nikles, L. Thevenaz, and P. A. Robert, "Simple distributed fiber sensor based on Brillouin gain spectrum analysis," *Opt. Lett.*, vol. 21, no. 10, pp. 758–760, May 1996.

[2] D. Zhou *et al.*, "Slope-assisted BOTDA based on vector SBS and frequency-agile technique for wide-strain-range dynamic measurements," *Opt. Exp.*, vol. 25, no. 3, pp. 1889–1902, 2017.

[3] X. Bao, M. DeMerchant, A. Brown, and T. Bremner, "Tensile and compressive strain measurement in the lab and field with the distributed Brillouin scattering sensor," *J. Lightw. Technol.*, vol. 19, no. 11, pp. 1698–1704, Nov. 2001.

[4] L. Zou, X. Bao, V. S. Afshar, and L. Chen, "Dependence of the Brillouin frequency shift on strain and temperature in a photonic crystal fiber," *Opt. Lett.*, vol. 29, no. 13, pp. 1485–1487, Jul. 2004.

[5] T. Horiguchi, K. Shimizu, T. Kurashima, M. Tateda, and Y. Koyamada, "Development of a distributed sensing technique using Brillouin scattering," *J. Lightw. Technol.*, vol. 13, no. 7, pp. 1296–1302, Jul. 1995.

[6] T. R. Parker, M. Farhadiroushan, R. Feced, V. A. Handerek, and A. J. Rogers, "Simultaneous distributed measurement of strain and temperature from noise-initiated Brillouin scattering in optical fibers," *IEEE J. Quantum Electron.*, vol. 34, no. 4, pp. 645–659, Apr. 1998.

[7] W. Zou, Z. He, and K. Hotate, "Complete discrimination of strain and temperature using Brillouin frequency shift and birefringence in a polarization-maintaining fiber," *Opt. Exp.*, vol. 17, no. 3, pp. 1248–1255, Feb. 2009.

[8] X. Bao and L. Chen, "Recent progress in distributed fiber optic sensors," *Sensors*, vol. 12, no. 7, pp. 8601–8639, Jun. 2012.

[9] Y. Mizuno, W. Zou, Z. He, and K. Hotate, "Proposal of Brillouin optical correlation-domain reflectometry (BOCDR)," *Opt. Exp.*, vol. 16, no. 16, pp. 12148–12153, Aug. 2008.

[10] H. Naruse and M. Tateda, "Trade-off between the spatial and the frequency resolutions in measuring the power spectrum of the Brillouin backscattered light in an optical fiber," *Appl. Opt.*, vol. 38, no. 31, pp. 6516–6521, Nov. 1999.

[11] M. A. Soto and L. Thévenaz, "Modeling and evaluating the performance of Brillouin distributed optical fiber sensors," *Opt. Exp.*, vol. 21, no. 25, pp. 31347–31366, Dec. 2013.

[12] Y. Takushima and K. Kikuchi, "Spectral gain hole burning and modulation instability in a Brillouin fiber amplifier," *Opt. Lett.*, vol. 20, no. 1, pp. 34–36, Jan. 1995.

[13] L. Stépien, S. Randoux, and J. Zemmouri, "Origin of spectral hole burning in Brillouin fiber amplifiers and generators," *Phys. Rev. A*, vol. 65, no. 5, May 2002, Art. no. 053812.

[14] S. Randoux and J. Zemmouri, "Comment on "Observation of inhomogeneous spectral broadening of stimulated brillouin scattering in an optical fiber"," *Phys. Rev. Lett.*, vol. 88, no. 2, Dec. 2001, Art. no. 029401.

[15] Y. Li, X. Bao, Y. Dong, and L. Chen, "A novel distributed Brillouin sensor based on optical differential parametric amplification," *J. Lightw. Technol.*, vol. 28, no. 18, pp. 2621–2626, Sep. 2010.

[16] R. W. Boyd. *Nonlinear Optics*. New York, NY, USA: Academic, 2003.

[17] C. H. Dong, S. Zhen, C. L. Zou, Y. L. Zhang, W. Fu, and G. C. Guo, "Brillouin-scattering-induced transparency and non-reciprocal light storage," *Nat. Commun.*, vol. 6, 2015, Art. no. 6193.

[18] J. H. Kim, M. C. Kuzyk, K. Han, H. Wang, and G. Bahl, "Non-reciprocal Brillouin scattering induced transparency," *Nat. Phys.*, vol. 11, no. 3, pp. 1797–1798, 2014.

[19] B. Peng, S. K. Özdemir, W. Chen, F. Nori, and L. Yang, "What is and what is not electromagnetically induced transparency in whispering-gallery microcavities," *Nat. Commun.*, vol. 5, 2014, Art. no. 5082.